ATP- and voltage-dependent electro-metabolic signaling regulates blood flow in heart

Guiling Zhao[a,1], Humberto C. Joca[a], Mark T. Nelson[b,c,1], and W. Jonathan Lederer[a,1]

[a]Laboratory of Molecular Cardiology, Center for Biomedical Engineering and Technology, Department of Physiology, University of Maryland School of Medicine, Baltimore, MD 21201; [b]Department of Pharmacology, The University of Vermont, Burlington, VT 05405; and [c]Division of Cardiovascular Sciences, The University of Manchester, Manchester M13 9PL, United Kingdom

Contributed by Mark T. Nelson, February 7, 2020 (sent for review December 19, 2019; reviewed by Heping Cheng and L. Fernando Santana)

Local control of blood flow in the heart is important yet poorly understood. Here we show that ATP-sensitive K^+ channels (K_{ATP}), hugely abundant in cardiac ventricular myocytes, sense the local myocyte metabolic state and communicate a negative feedback signal-correction upstream electrically. This electro-metabolic voltage signal is transmitted instantaneously to cellular elements in the neighboring microvascular network through gap junctions, where it regulates contractile pericytes and smooth muscle cells and thus blood flow. As myocyte ATP is consumed in excess of production, $[ATP]_i$ decreases to increase the openings of K_{ATP} channels, which biases the electrically active myocytes in the hyperpolarization (negative) direction. This change leads to relative hyperpolarization of the electrically connected cells that include capillary endothelial cells, pericytes, and vascular smooth muscle cells. Such hyperpolarization decreases pericyte and vascular smooth muscle $[Ca^{2+}]_i$ levels, thereby relaxing the contractile cells to increase local blood flow and delivery of nutrients to the local cardiac myocytes and to augment ATP production by their mitochondria. Our findings demonstrate the pivotal roles of local cardiac myocyte metabolism and K_{ATP} channels and the minor role of inward rectifier K^+ (Kir2.1) channels in regulating blood flow in the heart. These findings establish a conceptually new framework for understanding the hugely reliable and incredibly robust local electro-metabolic microvascular regulation of blood flow in heart.

ATP-sensitive potassium channel | heart | pericyte | capillary | electro-metabolic signaling

The efficiency and spatiotemporal management of cardiac blood flow appear to be perfectly matched to the metabolic needs of the heart at all times throughout the lifetime. This conclusion is supported by two observations. First, the heart extracts the maximum amount of oxygen from the circulating blood at all blood flows, as measured by the arteriovenous partial pressure of oxygen (pO_2) difference (1). This means that wherever blood flow in the heart is directed by the network of vascular valves and switches, it is needed by the tissue and for its oxygen and energy stores to make ATP. Second, each ventricular myocyte has an astoundingly small reserve of high energy phosphate (i.e., ATP and creatine phosphate), yet works for many decades (and often a life-time) without running out.

What constitutes "an astoundingly small reserve"? There are intracellular energetic reserves to support only 10 s to ~1 min of activity should cellular ATP production stop at times of high demand (2, 3). This means that regional (i.e., local) consumption of ATP is restored by the vascular network rapidly and accurately in response to uncertain ongoing and variable consumption. Therefore, it is surprising that such a well-tuned consumption and supply network is so poorly understood with respect to the overall mechanism of action. Importantly, however, multiple elements have been identified, each of which can contribute to the regulation of blood flow in the myocardium. These include adenosine (4), extracellular K^+ (5), H^+ (6), nitric oxide (7), reactive oxygen species (8), H_2S (9), and others that are presented in recent reviews (10, 11). While each may contribute to the process, an overarching hypothesis that provides a mechanistic link between anatomy and physiology is missing. This grand vision needs to be able to accommodate the aforementioned modulators of blood flow as well.

Here we report evidence to support a virtually instantaneous and highly local feedback control system centered on individual myocytes and their local environment. We have identified and characterized core features of "electro-metabolic signaling" in the heart. This mechanism focuses on the contracting ventricular myocytes, which consume the largest fraction of energy in the heart, and includes their neighboring microvascular components, including capillaries, pericytes, and vascular smooth muscle cells. Evidence presented here shows that the ventricular myocytes provide abundant metabolic sensors in the form of sarcolemmal K_{ATP} channels (12). When activated by a drop in $[ATP]_i$ and a rise in $[ADP]_i$ and possibly other modulators, these K_{ATP} channels open. By opening, the K_{ATP} channels hyperpolarize the ventricular myocytes and enable them to inject hyperpolarizing current into their local capillary endothelial cells through gap junctions. These capillaries can thereby communicate upstream electrically to hyperpolarize and relax contractile pericytes on capillaries and on small arterioles and to relax smooth muscle cells surrounding small arterioles and thus increase blood flow (13). The effect is very rapid and local.

Results

Our examination of blood flow in the heart makes use of a mouse papillary muscle preparation (14) taken from the right ventricle, as shown in Fig. 1 and described in *Materials and Methods*. The small

Significance

The ATP-sensitive K^+ channel (K_{ATP}) is a metabolite sensor that transduces the myocyte metabolic state into an electrical signal. Our studies show that this electro-metabolic signaling mechanism underlies the regulation of local blood flow in the heart through its actions on the contractile elements of the microvasculature. In addition, the efflux of K^+ supports this mechanism by its action on the capillary endothelial inward rectifier K^+ (Kir2.1). These findings establish a conceptually new framework for understanding the hugely reliable and incredibly robust local electro-metabolic microvascular regulation of blood flow in the heart.

Author contributions: G.Z., H.C.J., M.T.N., and W.J.L. designed research; G.Z. performed research; G.Z. and H.C.J. analyzed data; G.Z. interpreted data and prepared the figures; and G.Z. and W.J.L. wrote the paper.

Reviewers: H.C., Peking University; and L.F.S., UC Davis Health.

The authors declare no competing interest.

See online for related content such as Commentaries.

[1]To whom correspondence may be addressed. Email: gzhao@som.umaryland.edu, Mark.Nelson@uvm.edu, or jlederer@som.umaryland.edu.

This article contains supporting information online at https://www.pnas.org/lookup/suppl/doi:10.1073/pnas.1922095117/-/DCSupplemental.

First published March 13, 2020.

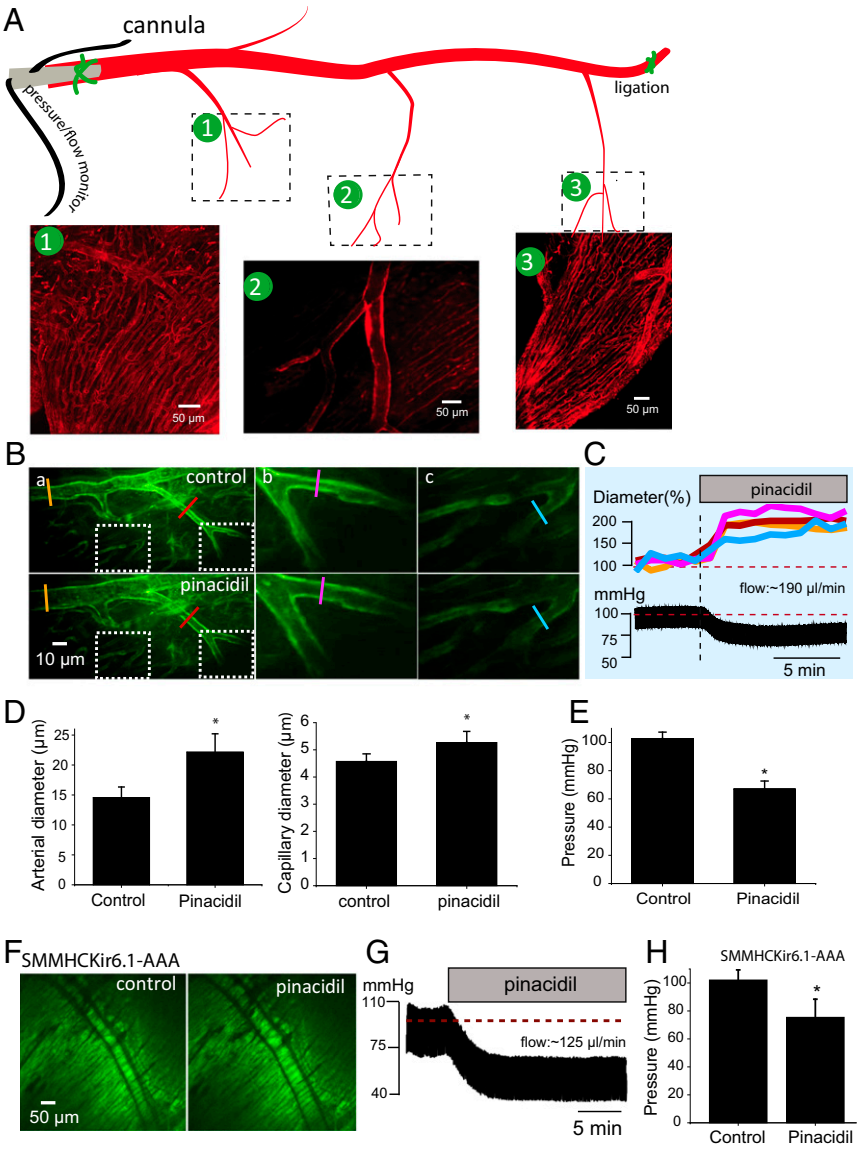

Fig. 1. Ventricular myocyte K_{ATP} opening increases coronary arterial blood flow. (*A*) Diagram of the experimental working model used in this study. The septal artery of mouse heart right papillary muscle was perfused using a fire-polished glass cannula. Tyrode's solution was perfused into the septal artery with either constant flow or constant pressure that was controlled using a pressure servo controller with a peristaltic pump. The flow rate of the solution and the arterial perfusion pressure were monitored simultaneously. When applicable, WGA conjugated with Alexa Fluor 633 or 488 was included in the luminal solution to visualize the vascular trees and capillary bed. The distal end of the septal artery was ligated to ensure sufficient perfusion to the papillary muscle and related tissues. The framed areas show the regions in which the images (1 to 3) were obtained. Images 1, 2, and 3 were obtained using confocal (1, 3) or spinning disk confocal (2) microscopy showing the capillaries and arterioles in the framed areas. (*B*) An example of the arteriole and capillary diameter changes with the luminal administration of pinacidil, a K_{ATP} opener. (*B*, *b* and *c*) Zoom-in views of the boxed areas in *B*, *a*. (*C*) Time course of the changes in arterial pressure (*Lower*) along with the changes in arteriole and capillary diameters (*Upper*). The line color in *C* reflects the diameter of the vessels highlighted with the same color in *B*. (*D*) Summary data showing the changes in arterial and capillary diameters caused by pinacidil ($n = 25$ for arterioles; $n = 4$ for capillaries). (*E*) Summary data showing the change in arterial pressure caused by pinacidil. $n = 10$ mice. $^*P < 0.05$ vs. control, paired *t* test. (*F*) Representative images showing the effect of pinacidil on arterial diameter in papillary muscle from an SMMHCKir6.1-AAA mouse, in which the K_{ATP} function was eliminated in smooth muscle. (*G*) Original trace showing the effect of pinacidil on the septal arterial luminal pressure in an SMMHCKir6.1-AAA mouse. (*H*) Summary data showing the effect of pinacidil on arterial pressure in SMMHCKir6.1-AAA mice. $n = 3$ mice. $^*P < 0.05$ vs. control, paired *t* test.

septal artery (~100 to 200 μm in diameter) is cannulated and pressurized as shown diagrammatically in Fig. 1*A*. Feedback control systems enable us to control either flow or perfusion pressure in the cannulated artery and to measure the other (i.e., pressure or flow) (Fig. 1 *B* and *C* and *SI Appendix*, Fig. S1 *B–D*). The insets in Fig. 1*A* show confocal images of three branches from the central cannulated small artery. Alexa Fluor 633- (or 488-) conjugated wheat germ agglutinin (WGA) was used to stain the vessels, including arterioles and capillaries. The microvasculature appears to fill the volume of the tissue but is actually tightly interdigitated with other cells in the tissue, primarily ventricular myocytes, as shown in *SI Appendix*, Fig. S1*A*. The physiological function of the preparation was demonstrated by applying pressure and perfusing the vasculature with the vasoconstrictor endothelin 1 (ET-1; 10 nM) from the arterial lumen, as shown in *SI Appendix*, Fig. S1 *B–D*. An important observation in terms of our investigation of blood flow control comes from the action of the application of drugs that open K_{ATP} channels (pinacidil and diazoxide; 100 μM) to the solution perfusing the cannulated papillary muscle artery (Fig. 1 *B–E* and *SI Appendix*, Fig. S2 *A–C*). Fig. 1 *B* and *C* show that the

opening of K_{ATP} channels by pinacidil leads to dilation of all components of the microvasculature (small arterioles and capillaries). Similar results were obtained from another K_{ATP} opener, diazoxide (*SI Appendix*, Fig. S2 *A–C*).

Both vascular endothelial cells and smooth muscle cells have K_{ATP} channels with Kir6.1 as the pore-forming subunit, while ventricular myocytes have K_{ATP} channels with both Kir6.2 and Kir6.1 as pore-forming subunits (15–17). Therefore, to identify whether the vasculature K_{ATP} channels or the ventricular myocyte K_{ATP} channels underlie the vasodilation observed in Fig. 1 *B–E*, we examined the vasculature in mice with a mutated smooth muscle Kir6.1 pore-forming subunit (SMMHCKir6.1-AAA mice), and the function of K_{ATP} was abolished, as shown in *SI Appendix*, Fig. S2*D* (16). Kir6.1 appears to be the pore-forming unit of the K_{ATP} channel in vascular smooth muscle cells and coronary endothelial cells (15, 16, 18). While brain pericytes have Kir6.1, cardiac pericytes appear to have no K_{ATP} channels (19). Here we show that the decrease of arterial perfusion pressure and vasodilation in response to pinacidil are unchanged in the Kir6.1 mutated mouse compared with the wild-type control (Fig. 1 *F–H*). Thus, the critical K_{ATP} channels that are activated by pinacidil are not in the vasculature and specifically not in the smooth muscle cells or pericytes. This finding raises the question of how hyperpolarization signals from the ventricular myocytes affect contractile elements in the local vasculature.

The simplest and fastest connection between ventricular myocytes and the vasculature would be an electrical connection through gap junctions (20). Such gap junctions would need to be present and patent from ventricular myocytes to capillary endothelial cells and thus to capillary pericytes and on to both neighboring endothelial cells in the small end arterioles and vascular smooth muscle cells. All such gap junctions have been reported in diverse tissues and cells (13, 21–23) except those between ventricular myocytes and capillary endothelial cells, which have occasionally been noted but more anecdotally (20). To test this possibility, freshly isolated rat ventricular myocytes were put in a primary coculture with human cardiac microvascular endothelial cells, as shown in Fig. 2*A*. Gap junctions, known to be present in endothelial cells and in ventricular myocytes, could in principle establish critical connections between the two very different cell types. Ventricular myocytes are replete with connexin (Cx) 43 and Cx45 (24), while capillary endothelial cells normally contain Cx40, Cx43, and Cx37 (25, 26). If the distinct gap junction types could readily establish a connection between the two cell types, such a connection would permit current to flow between connected cells and would also permit molecules ~1,000 Da (27) and smaller to readily diffuse from one cell type to the other. Thus, we used the

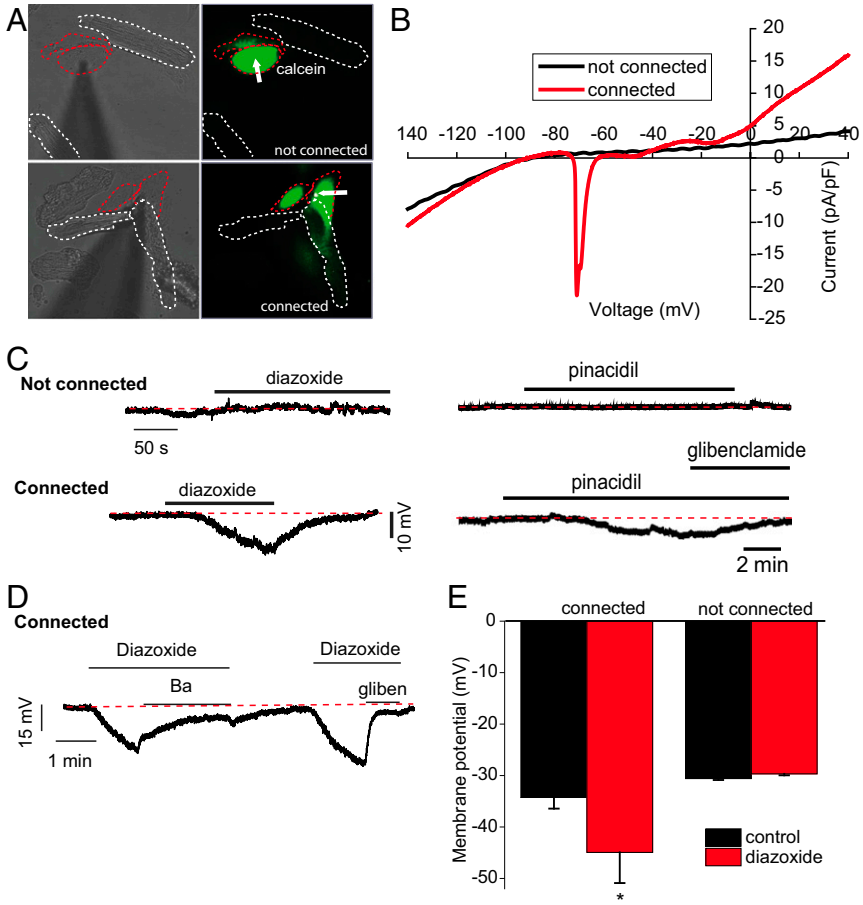

Fig. 2. Rat ventricular myocyte K_{ATP} openings hyperpolarize the membrane potential of cultured human capillary endothelial cells. (*A*) Representative images showing the physical relationship between ventricular myocytes and the neighboring endothelial cells by monitoring the calcein fluorescence diffusion from endothelial cells to ventricular myocytes in coculture. Calcein was included in patch pipettes. (*B*) Whole-cell currents with voltage ramps showing the transient inward current (TIC) in an endothelial cell connected to a rat ventricular myocyte. (*C*) Diazoxide (*Left*) and pinacidil (*Right*) induced membrane hyperpolarization only in the endothelial cells connected to the paired ventricular myocyte (*Bottom*). (*D*) Diazoxide-induced membrane hyperpolarization seen in a connected myocyte-endothelial cell pair is blocked by 100 μM Ba^{2+} and 100 μM glibenclamide. (*E*) Summary data showing the effect of diazoxide on the endothelial cell membrane potential in coculture (n = 4 and 9 for connected and nonconnected cells, respectively).

fluorescent marker calcein salt (623 Da) in a patch clamp intracellular solution to determine whether both current and calcein could pass from one cell type to the other. Fig. 2*A* shows outlines of the two cell types in close contact (red, endothelial cells; white, cardiac ventricular myocytes). The top pair of images show that when the cells are not electrically connected, the calcein injected into the patch-clamped endothelial cells does not enter the ventricular myocytes. The bottom pair of images show that when the endothelial cells and ventricular myocytes are electrically connected, the calcein moves from the endothelial cells to the ventricular myocytes after injection into the endothelial cells. Fig. 2*B* shows the evidence of current injected from the cardiac myocyte into the endothelial cell when the cell pair is connected. The black line reflects the current-voltage relationship of the endothelial cell alone when a voltage ramp from −140 to +40 is applied. The zero-current potential ("reversal potential") of the endothelial cell is approximately −90 mV and does not change when it is linked to the ventricular myocyte (red line) by one or more gap junctions ("connected"). In clear contrast, as the voltage ramp moves from −140 to +40, the red line shows the distinctive and different shape at around −70 mV. Here the current-voltage relationship produced by the connected hybrid pair of cells that includes an endothelial cell and a ventricular myocyte, shows a spike of inward current. The spike of inward (depolarizing) current at around −70 mV reflects the activation of sodium and calcium channels in the ventricular myocyte and shows the depolarizing current injected into the endothelial cell. The spike of inward current disappears when the myocyte is physically removed (*SI Appendix*, Fig. S3 *A* and *B*). In the connected cell pair, there is also a small but clear increased inward and outward current at a very negative and a very positive potential that reflects current injected into the endothelial cell mainly due to potassium channels in the ventricular myocytes. This approach provides compelling support for the connectivity of the ventricular myocytes to the capillary endothelial cells, as suggested by the data in Fig. 1.

To examine the possible role of endothelial cells in contributing to the vasodilation produced by the K_{ATP} channel opener pinacidil shown in Fig. 1, we carried out current clamp experiments. The time course of changes in endothelial cell membrane potential (V_m) was measured when the endothelial cells were either connected or not connected to ventricular myocytes (Fig. 2 *C*–*E*). We saw no change in endothelial cell V_m when the cells were not connected to ventricular myocytes (from −30.4 ± 2.9 mV to −29.4 ± 2.8 mV; Fig. 2 *C* and *E*). However, when the endothelial cells were connected to ventricular myocytes by gap junctions, application of K_{ATP} channel activators (e.g., diazoxide 500 μM, pinacidil 100 μM) produced a hyperpolarization in the endothelial cells that could be blocked by Ba^{2+} (100 μM) or a K_{ATP} channel inhibitor (e.g., glibenclamide 100 μM) (Fig. 2 *C*–*E*). The results shown in Fig. 2 indicate that the activation of K_{ATP} channels in the ventricular myocytes underlies the vasodilation observed in the intact tissue produced by pinacidil shown in Fig. 1. Unlike in rat ventricular myocytes (12, 28) (*SI Appendix*, Fig. S4) or capillary endothelial cells from guinea pig heart (29), K_{ATP} openers do not change whole cell current or membrane potential in human microvascular endothelial cells, as shown in *SI Appendix*, Fig. S5. Taken together, these results show that the vasodilation caused by pinacidil and diazoxide is not due to K_{ATP} channels in the endothelial cells or in vascular smooth muscle cells or pericytes.

In addition to the gap junction-dependent hyperpolarizing effect of the activation of cardiac myocyte K_{ATP} channels on the nearby microvasculature shown in Figs. 1 and 2, we show an additional interesting result in Fig. 3. Here a distinct action of elevated extracellular potassium on cardiac microvascular endothelial cells is revealed. Elevated $[K^+]_o$ is routinely used to depolarize cells (30); however, Fig. 3 shows a circumstance in which an increase in $[K^+]_o$ hyperpolarizes the membrane potential in cultured human capillary endothelial cells. Importantly, at potentials close to the putative resting potentials (−30 to −40 mV) of endothelial cells, an increase in extracellular potassium (e.g., to ∼15 mM) can hyperpolarize the membrane potential of the endothelial cells, as is shown in the current clamp (at current 0) measurement of V_m reported in Fig. 3 *A* and *B*. The voltage clamp measurement at −40 mV shows the hyperpolarizing current that underlies this hyperpolarization. Both hyperpolarization effects of $[K^+]$ are blocked by Ba^{2+} (100 μM), a feature consistent with the inward rectifier K^+ channel (Kir2.1), a critical component of functional Kir in capillary endothelial cells (13). This unexpected action of elevated $[K^+]_o$ occurs because in microvascular endothelial cells, Kir2.1 has N-shaped current-voltage relationships that "cross over," as shown in Fig. 3 *D* and *E*, when $[K^+]_o$ increases from 5 mM to 15 mM (Fig. 3 *E*, *Inset*). At −40 mV, there is a clear increase in outward (hyperpolarizing) current as $[K^+]_o$ increases from 5 mM to 15 mM (Fig. 3 *C* and *E*).

These observations are supported by the significant differences in current shown in Fig. 3*F*, which demonstrate the differences in elevated $[K^+]_o$-activated current at −40 mV (outward, hyperpolarizing current) versus at −140 mV (inward, depolarizing current). Thus, insofar as K_{ATP} are activated and other repolarizing sarcolemmal K^+ channels are activated in ventricular myocytes, there will be an increase in $[K^+]_o$ surrounding the capillary endothelial cells, which will tend to produce a vasodilating hyperpolarization (5, 13, 31). We conclude that the ventricular myocytes produce hyperpolarizing current when K_{ATP} channels are activated and this hyperpolarizing current is injected into the "microvascular network" to increase microvascular diameter and increase blood flow. This significant action is augmented by the local increase in $[K^+]_o$ outside of the capillary endothelial cells that tightly surround the ventricular myocytes when the endothelial cell membrane potential is around −40 mV.

A critical element in the observations that we have presented is the electrical connectivity between and among the cellular elements. It is through this electrical signaling that the metabolic state of a specific ventricular myocyte can signal to nearby upstream capillaries, pericytes, smooth muscle cells, and arterioles that it needs more oxygen and food stock to operate. This is the signaling pathway that underlies electro-metabolic coupling between the heart muscle and coronary vasculature. We have shown that the signaling system works, but it is also important to show key anatomic elements in the signaling pathway. Here we provide evidence that ventricular myocytes are electrically connected to capillary endothelial cells and that endothelial cells are electrically connected to pericytes and vascular smooth muscle in the small arteries and end arterioles.

As noted above, we have already provided functional evidence supporting this chain of electrical signaling in heart tissue. Here we examine the presence of the electrical connections made by means of gap junctions that involve Cx43. The images in Fig. 4 are whole-tissue mounts of fixed tissue that had been perfused and then fixed and permeabilized. We use antibodies and fluorescence tags to identify endothelial cells (Fig. 4*A*, *a*; WGA, magenta), ventricular myocytes (Fig. 4*A*, *b*; α-actinin, blue), and pericytes (Fig. 4*A*, *c*; NG2, red). Fig. 4 shows the presence of Cx43 as gap junction patches (green) that run in a linear organization along the surface membrane of the capillary endothelial cells and are in the appropriate locations to connect them with both ventricular myocytes and pericytes (Fig. 4*A*, *g*, white arrows). This same figure also shows the presence of Cx43 in the pericytes that decorate the capillaries and arterioles (Fig. 4*A*, *h* and *i*, yellow arrows). The zoomed-in images in Fig. 4*B* clearly show the colocalization of Cx43 with myocytes, WGA, and NG2 (Fig. 4*B*, *e*–*k*, white and yellow arrows). Higher power image in Fig. 4*B* demonstrates few yet clear capillary wall location of gap junctions (Fig. 4 *B*, *g* and *k*). These gap junctions (Cx43) may link pericytes to capillary endothelial cells, pericytes to cardiac myocytes, or capillary endothelial cells to cardiac myocytes. We highlight some of these locations in Fig. 4*C*.

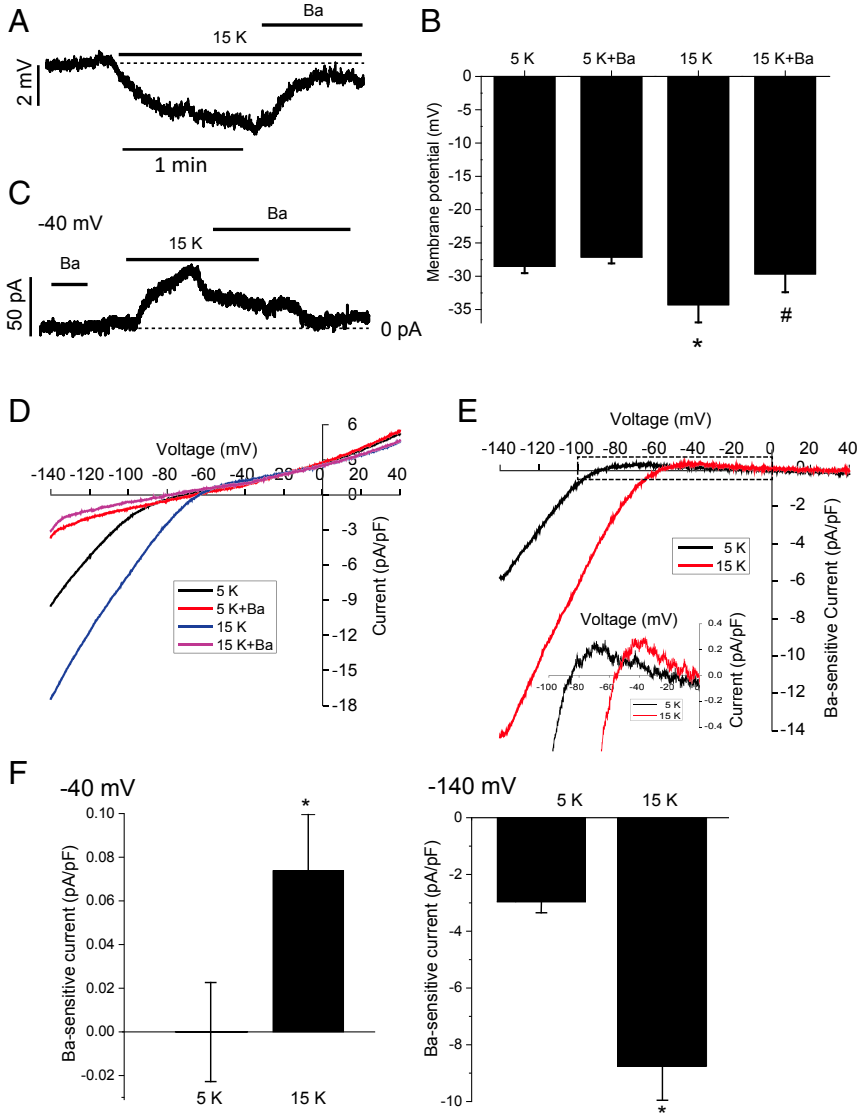

Fig. 3. Elevated $[K]_o$ induces endothelial cell membrane hyperpolarization by activating Kir2.1. (*A*) Representative whole-cell current-clamp recording showing that elevated $[K]_o$ (15 mM) hyperpolarizes an endothelial cell by a Ba^{2+}-sensitive current. (*B*) Summary data showing Ba^{2+}-sensitive hyperpolarization of the membrane potential produced by 15 mM $[K]_o$ ($n = 8$ cells). *$P < 0.05$ vs. 5 K; #$P < 0.05$ vs. 15 K, paired *t* test. (*C*) Representative whole-cell voltage-clamp recording showing a Ba^{2+}-sensitive outward current from an endothelial cell elicited by elevated $[K]_o$ (15 mM) at −40 mV. Recordings in *A* and *C* are from the same cell. (*D*) Current traces from voltage ramp experiments showing that $[K]_o$ (15 mM) increases Ba^{2+}-sensitive whole-cell current (due to Kir2.1). (*E*) Ba^{2+}-sensitive currents produced by voltage ramps in *D*. (*Inset*) Zoom-in view of the region marked by the dashed box showing that $[K]_o$ (15 mM) induces an outward current over a voltage range of −50 to −10 mV. (*F*) Summary data showing the effect of $[K]_o$ on Kir2.1 current at −40 mV and −140 mV. $n = 15$ cells. *$P < 0.05$ vs. 5 K.

Additional staining of cardiac myocytes using α-actinin with Cx43 shows the presence of gap junction patches at both the intercalated disk area and the lateral side of the myocytes (Fig. 4 *A* and *B*, *f*). Matching those lateral lines of gap junctions are the paths of capillary endothelial cells that are identified by WGA (Fig. 4*B*, *g*, magenta). This image and the zoomed-in images are consistent with the demonstrated electrical connectivity between myocytes and endothelial cells demonstrated in Fig. 2 *A*–*E*. These images provide support for the presence of the anatomic hardware needed for electrical connectivity. Figs. 1, 2, and 6 show that there are functional consequences of this connectivity.

Here we describe a physiological working model that links the metabolic need of cardiac myocytes to blood flow through intercellular electrical and chemical communication on a beat-to-beat basis. While all the aforementioned experiments were performed in the quiescent state to minimize the effect of movement on the current and arterial/capillary diameter measurements, the next test was carried out on the electrically stimulated preparations to mimic the physiological state. As shown in Fig. 5 *A* and *B*, when the papillary muscle was electrically stimulated (50 V for 2 ms) with different frequencies (over the range 1 to 12 Hz, to reflect the range of electrical activity common in mice at 37 °C), the perfusion pressure was different at a constant flow (~150 μL per minute). In brief, when the pacing frequency was increased, the perfusion pressure needed to maintain constant flow decreases (Fig. 5 *A* and *B*). This is consistent with the dilation of arteries at the higher stimulation rate in physiological ranges (32). When the papillary muscle was paced at a lower rate (1 Hz), the K_{ATP} opener pinacidil (100 μM) led to the decrease in arterial perfusion pressure (Fig. 5*C*). In addition, in the presence of pinacidil, the arterial perfusion pressure barely changed when the pacing rate was increased from 1 Hz to 8 Hz. When the papillary muscle was paced

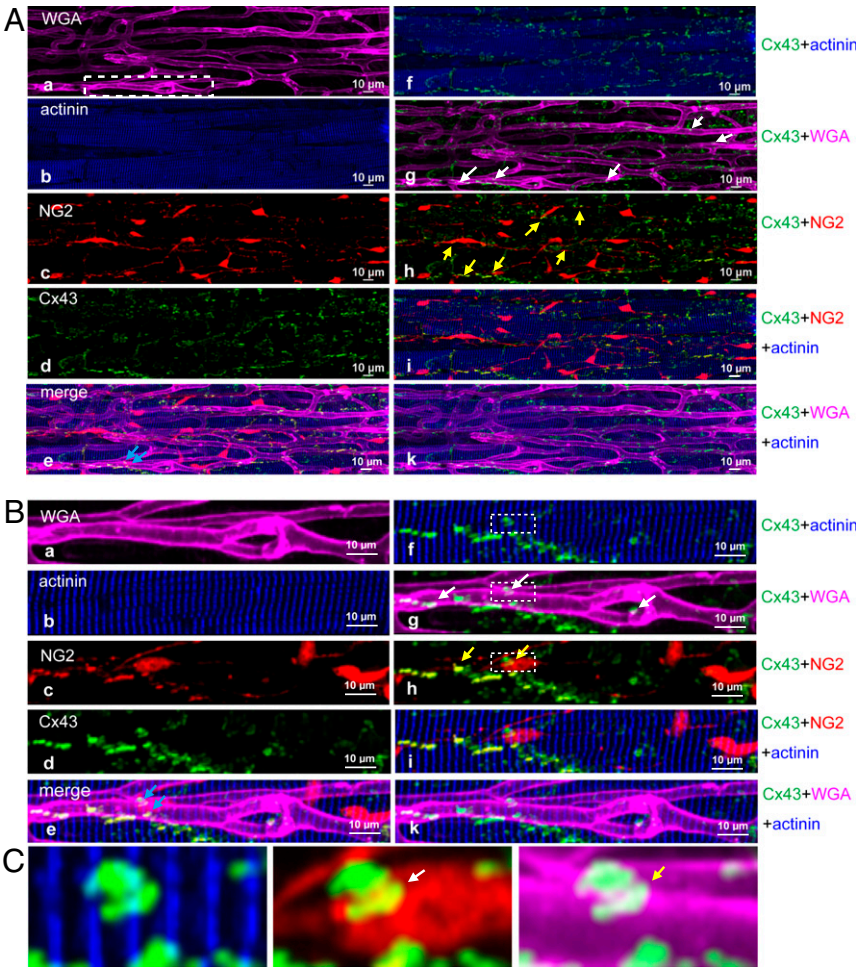

Fig. 4. The intercellular connections among cardiac myocytes, capillary endothelial cells, and pericytes in mouse right papillary muscle. (*A*) Immunostaining showing Cx43 in and between capillary endothelial cells (white arrows), cardiac myocytes, and pericytes (yellow arrows). Cx43 connections between myocytes and capillary endothelial cells are also observed (cyan arrows). See text in the *Results* section for details. (*B*) Expanded view from the white box in *A*, *a*. (*C*) Further enlarged regions from *B* (boxed area) showing a gap junction-rich region between ventricular myocytes (*Left*), a Cx43-rich region aligned with myocytes and capillary endothelial cells (white arrow) (*Middle*), and apparent Cx43-rich junctions overlapping with capillary endothelial cells and pericytes (yellow arrow) (*Right*). All images were collected using Z-stack with a step of 0.325 μm. These images are Z-projections of the maximum intensity.

at 8 Hz, a frequency close to the normal physiological rate for mice, glibenclamide (100 μM) caused an increase in arterial perfusion pressure when flow was maintained at a constant level (Fig. 5*D*). These data demonstrate that as metabolic demand increases with an elevation of cardiac electrical activity to a physiological level (8 Hz), cardiac K_{ATP} channels open to engage the local capillary network to signal blood delivery. Thus, the effect of the K_{ATP} channel agonist decreases and the effect of the K_{ATP} channel antagonist glibenclamide increases. This also suggests that K_{ATP} channels in the heart are normally partially activated (i.e., open) under physiological conditions (33).

Discussion

Electro-Metabolic Signaling System in Heart. Here we present a new blood flow control system for the heart, dubbed "electro-metabolic signaling" (Fig. 6). Our findings integrate diverse features, some partly established by past work, but together all the elements are linked with new evidence presented here that provides a robust solution to physiological blood flow regulation in mammalian heart. We directly address the question of the apparent overabundance of K_{ATP} channels in ventricular myocytes (*SI Appendix*, Fig. S4) (28) as an adaptive solution that enables rapid "upstream" electrical regulation of blood flow. Furthermore, we identify the key roles played by the cellular elements (myocytes, capillary and vascular endothelial cells, pericytes, and vascular smooth muscle cells). Together, the components of this electro-metabolic signaling system enable the heart to optimize oxygen extraction and blood flow nearly instantaneously to meet dynamic real-time metabolic needs of the myocytes. An additional key conceptual element is embodied in the microvascular electrical network (34). This physiological mechanism is the core process by which blood flow is regulated in heart as orchestrated by ventricular myocytes. As the heart rate and workload vary with exercise, physical work, and biological stress, electrical signals are sent upstream using the capillary and vascular endothelium as a communication network (13).

Importantly, electro-metabolic signaling does not negate additional processes already characterized that also influence and tune blood flow (4, 7, 8, 10, 35). A broadly important and central finding for which we provide important evidence is the electrical connection from myocytes to capillary endothelial cells that enables the end-user myocytes to regulate the opening and closing of vascular flow valves composed of pericytes and vascular smooth muscle cells. Thus, even modest activation of the K_{ATP} channels (as can occur with a decrease in $[ATP]_i$ or an increase in $[ADP]_i$) can inject a net hyperpolarizing current into the local

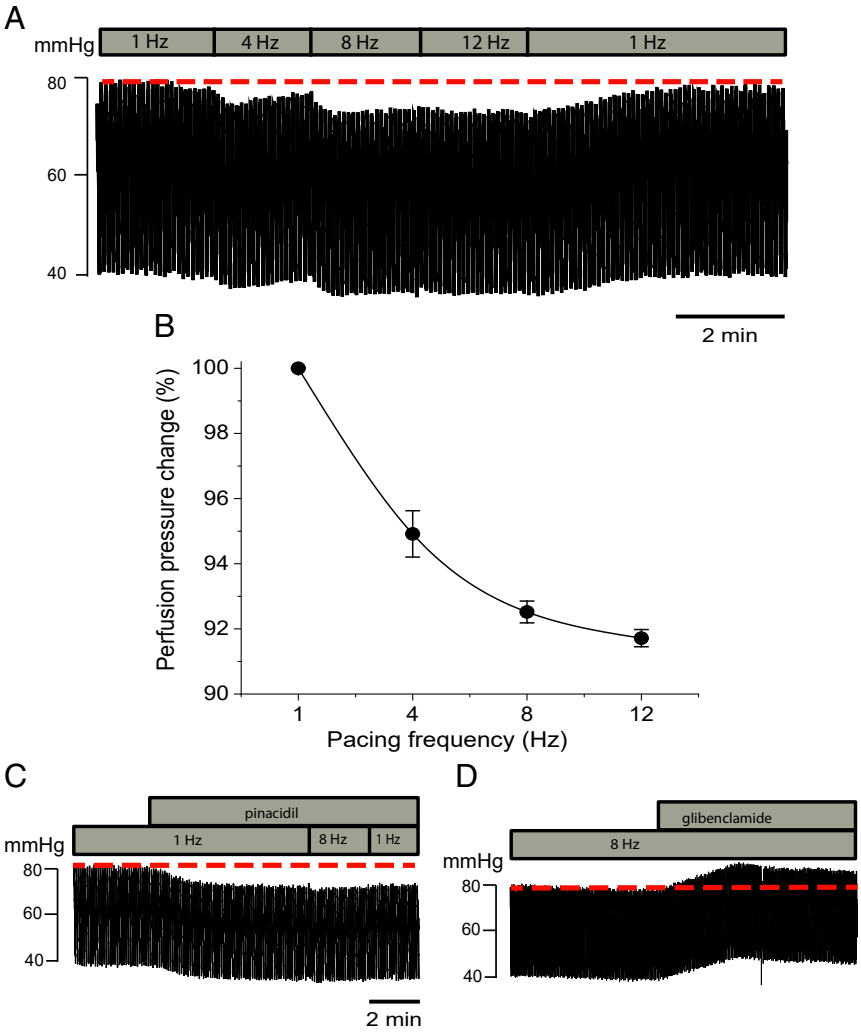

Fig. 5. K_{ATP} is partially activated (open) under physiological conditions and modulated by heart rate and work in papillary muscle. (*A*) Representative traces showing that increased pacing frequency (from 1 to 12 Hz) underlies vasodilation, as evidenced by a decrease in arterial perfusion pressure (when flow is constant). (*B*) Summary data showing the decrease in arterial perfusion pressure with an increase in pacing rate (when flow is constant). $n = 3$ mice. (*C* and *D*) Representative traces showing that pinacidil decreases arterial perfusion pressure at a low pacing rate (1 Hz), and that glibenclamide increases arterial perfusion pressure at a high (8 Hz) pacing rate (with constant flow). In the presence of pinacidil, an increase in pacing frequency from 1 Hz to 8 Hz does not change the arterial perfusion pressure (*C*) (with constant flow).

microvascular electrical network to minimally increase blood flow (28, 34). Thus, there is a wide sensitivity of the system so that it can respond to metabolic changes. In addition, it enables a massive ramp-up in its efficacy and responsiveness when $[ATP]_i$ drops more dramatically. While the primary mechanism is centered on the K_{ATP} channels of the cardiac myocytes, there is a secondary signaling pathway that is much smaller and depends indirectly on electrical activity and on the Kir2.1 of endothelial cells and its sensitivity to extracellular $[K^+]_o$. These elegant and flexible mechanisms provide a fundamental understanding for blood flow control in the heart. We discuss additional important features below, some of which are illustrated in Fig. 6.

While electro-metabolic signaling regulates blood flow in small regions of the heart as physiology demands, additional factors also influence the details of flow. For example, vasomotion, muscle compression, adrenergic and parasympathetic tone, and many other factors exert an influence on flow even while electro-metabolic signaling is operational (10, 11, 36). These factors work together. Electro-metabolic signaling is driven by the needs of the tissue and can compensate for any interferences with only a small phase lag, since the overarching control mechanism is regulated locally by the myocyte metabolic state and $[ATP]_i$ level within these cells.

Electro-Metabolic Signaling Is Local and Timely. In the absence of extensive energy stores in heart muscle and essential nonstop operation, blood flow is continuously critical to cardiac function. It serves to resupply the mitochondria with lipids, carbohydrates, and protein—the primary energy sources of the heart—to bring oxygen and remove waste products. The huge number of mitochondria rapidly convert raw food stock to ATP to maintain cardiac function, blood pressure, and regulate circulation. The large volume fraction of the heart that is mitochondrial reflects this critical balance. The tight control over the regulation of the blood flow appears new to many studying the balance between blood flow and energy consumption. The emergence of the critical roles of pericytes and small vessel smooth muscle is shown here (Fig. 6 *A* and *B*) and may appear novel (37); however, the early presentation and description of pericytes in capillaries dates back nearly 100 y (38). Here we provide evidence that as K_{ATP} channels in myocytes are activated by pinacidil, dilation of capillaries and small arterioles occurs (Fig. 1 *B*–*D*) due to pericytes and smooth muscle cells. We

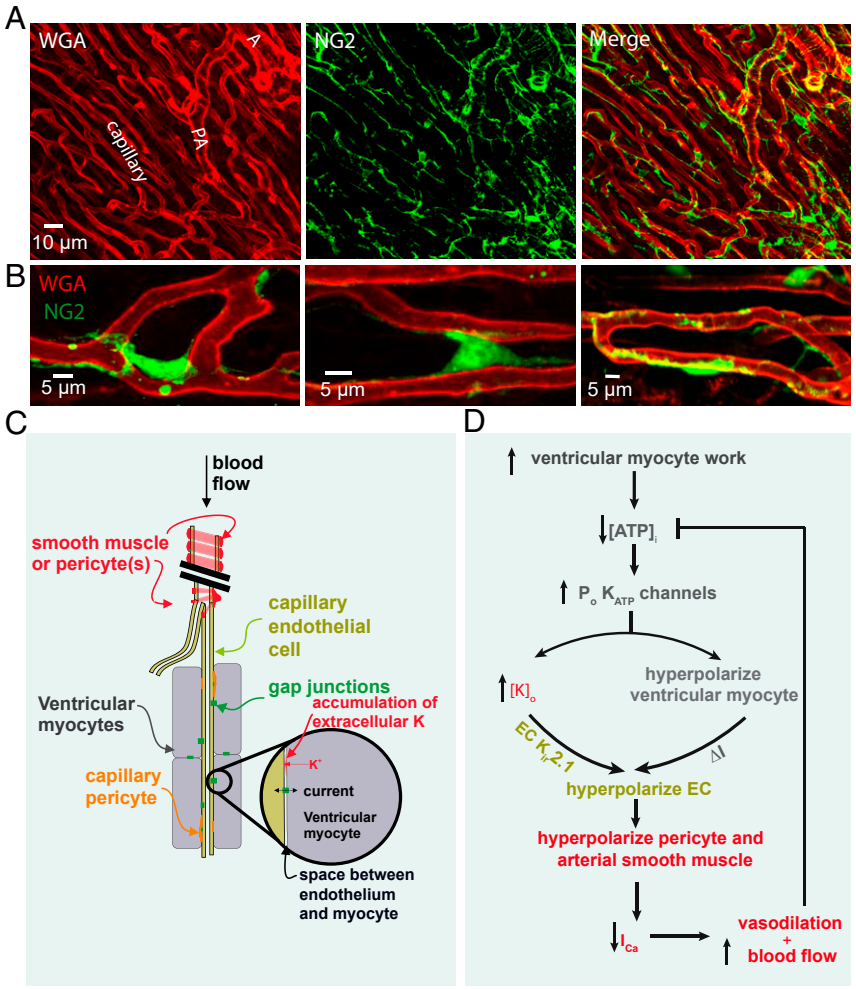

Fig. 6. Blood flow control mechanisms in the heart: electro-metabolic signaling. (*A*) Representative images from fixed tissue showing arteriole (A), pre-capillary arteriole (PA), capillaries (red, WGA), and pericytes (green, NG2) in mouse papillary muscle. (*B*) Zoomed- in images showing the structure of capillary pericytes (green, NG2) around the capillaries (red, WGA). These images clearly show that the capillary pericytes regularly span two or more capillaries with their processes. (*C*) Diagram of the structures involved in electro-metabolic regulation of blood flow in the heart. (*D*) Diagram showing the overall logic of electro-metabolic regulation of blood flow in the heart.

also show how pericytes wrap around the capillary endothelium next to myocytes and at small vessel junctions, enabling the dynamics of capillaries and arterioles and the regulation of their diameter and resistance to flow (Fig. 6 *A* and *B*). Thus, the hyperpolarization of the vascular network reduces Ca^{2+} influx to enhance blood flow, as reported previously (39).

The electro-metabolic signaling regulation is "super-local" with regard to the vascular components (capillary, pericytes, and vascular smooth muscle) and myocytes. They talk to one another electrically through gap junctions and chemically (Fig. 4). The extent of the communication in space is limited by the size of the signal, the "leakiness" of the electrical signal, and the organization of the network. The abundance of capillaries puts approximately one capillary per myocyte (on average) in cross-section, with an average capillary length of 50 to 100 microns. There appears to be approximately one pericyte per capillary (length between branch points). As shown in Fig. 6 *A* and *B*, the pericytes in both living and fixed tissues have a floppy cell body with spidery arms that wander around and along the surface of the capillary endothelial cell. The cell body may span the separation between neighboring capillaries or along the surface at the junction between several capillary junctions. Presumably, the narrowing of the capillary reflects contraction of the thin arms. The packing of contractile and vascular structures is organized so that electro-metabolic signaling regulation can work as illustrated in Fig. 6*C*. In 3D organization, this places five or six myocytes and capillaries around each myocyte.

Electro-metabolic signaling, a novel system conceptually, bundles direct metabolic sensing with blood flow regulation in a compact, spatially organized manner. The central elements in this mechanism and conceptual framework involve the local control of metabolic needs. The data presented here show how cardiac anatomy and molecular physiology enable the myocytes to rapidly sense local metabolic needs and instantly communicate these needs to the local upstream and neighboring vascular smooth muscle cells or pericytes (37, 40) through endothelial cells. When hyperpolarized electrically due to the consequences of downstream metabolic needs, the contractile cells relax to increase blood flow in a manner proportional to local downstream needs. At the core of the investigation is the electrically connected cardiac microvasculature that extends from the ventricular myocytes to their local capillaries and neighboring arterioles. The central features of this feedback control system are illustrated in Fig. 6*D*. The heart represents the ultimate biological development of a tightly controlled system, since at all flow rates it maximally extracts oxygen from the blood (1). Starting at the top of the diagram, work by the heart consumes ATP, and the decrease in $[ATP]_i$ proportionally

activates K_{ATP} channels and the efflux of K^+. The hyperpolarizing current of the K_{ATP} channels is injected into the electrical network (of endothelial cells, pericytes, and vascular smooth muscle cells), while the K_{ATP} channel and other increased K^+ channel K^+ efflux elevates the likelihood that Kir2.1 channels in the endothelium produce hyperpolarizing current directly (41). The hyperpolarization of pericytes and vascular smooth muscle cells reduces Ca^{2+} influx through Ca^{2+} channels, which relaxes the pericytes and vascular smooth muscle cells to increase blood flow (39, 42, 43). This serves to restore blood flow and oxygenate the myocytes, thereby making more ATP and removing waste products. While this clever system works brilliantly in the heart, Longden (13) recently showed that in the brain, repolarizing K currents produce a huge K^+ efflux to use the N-shaped Kir2.1 current-voltage curve as the dominate mechanism to produce vascular relaxation and increased blood flow.

Contribution of Ventricular Myocyte Membrane Potential (V_{vm}) to Capillary Endothelial Cell Potential (V_{cec}). The resting potential of the ventricular myocytes is approximately −80 mV and becomes as positive as approximately +40 mV during the action potential (AP). Thus, the time-averaged potential of the ventricular myocyte, $\bar{V}$, varies between approximately −60 mV to approximately −20 mV and depends primarily on the AP shape and the heart rate. The estimated V_{cec} is between −25 and −70 mV (29, 44). Whatever $\bar{V}$ may be, it will move in the negative direction as K_{ATP} channels in the ventricular myocytes are activated by the drop in $[ATP]_i$ within the ventricular myocytes (34, 45). Thus, activation of the K_{ATP} channels will shorten the AP of the myocytes (46, 47), leading to a time-averaged potential more negative and closer to E_K (the Nernst potential of K^+, approximately −90 mV). At any given value of $\bar{V}$, the current injected into the local vascular network from the local ensemble of ventricular myocytes depends on V_{cec} and the number and location of open gap junctions between the VMs and the CECs, the conductance of these gap junctions, as well as the effective local impedance. As a complex 3D dynamic network, it has not been possible for us to identify and measure these variables sufficiently to constrain a model of the system. Additional complexity comes from the interactions among all the neighboring local systems. Work in progress seeks to identify and measure all of these elements. Here we have presented data showing that each of the major components of the electro-metabolic systems exists and is modulated as described in the text and shown in Fig. 6. Together, the data shown provide evidence for electro-metabolic coupling as a system in the heart that regulates blood flow primarily by the effects of $[ATP]_i$ in myocytes with a modest component attributed by outward current activated by elevated $[K]^+$ bathing capillary endothelial cells. This elevated $[K^+]$ from the ventricular myocytes activates Kir in a region of its current-voltage (IV) curve that has a negative slope. However, the primary driver of blood flow control under the conditions tested is the $[ATP]_i$ in the ventricular myocytes.

Materials and Methods

Animal Handling and Preparation of Mouse Septum and Papillary Muscle. All animal care was provided in accordance with the guidelines of the University of Maryland Baltimore's Institutional Animal Care and Use Committee-approved protocols. Rats and mice were handled as described previously (48). NG2-DsRed mice were purchased from The Jackson Laboratory (catalog no. 008241). Tamoxifen-induced SMMHKir6.1-AAA mice were a gift from Dr. Colin G. Nichols, Washington University in St. Louis. The fresh heart of each euthanized mouse was surgically removed and placed into ice-cold Tyrode's solution containing the following components: 140 mM NaCl, 10 mM Hepes, 0.5 mM $MgCl_2$, 0.33 mM $NaHPO_4$, 5 mM glucose, 1.8 mM $CaCl_2$, and 5 mM KCl (pH 7.4 with NaOH), along with 30 mM 2,3-butanedione monoxime (BDM). After being cleaned of connective tissues, the heart was transferred into a Sylgard-coated prechilled (4 °C) chamber with Tyrode's solution containing 30 mM BDM. The heart was pinned down onto the Sylgard layer of the chamber. The free walls of both ventricles were removed. The septal artery was exposed and cannulated using a fire-polished bent glass pipette prefilled with Tyrode's solution. The pipette used to cannulate the septal artery was then connected to a pressurized line. The line was pressurized by a peristaltic pump (Living Systems Instrumentation) that was used to perfuse the artery when activated. A pressure transducer was used to measure the perfusion pressure. The flow rate (in μL/min) and arterial perfusion pressure (in mmHg) were digitized (Digidata 1322; Molecular Devices) and recorded using AxonScope (Molecular Devices). The vascular lumen perfusate was Tyrode's solution heated as it traversed the bath superfusate in a gas permeant tube. The superfusate contained a physiological saline solution (PSS; containing 112 mM NaCl, 5 mM KCl, 1.2 mM $MgSO_4$, 1.2 mM NaH_2PO_4, 24 mM $NaHCO_3$, 10 mM glucose, and 1.8 mM $CaCl_2$) was maintained at 35 to 37 °C with a heater and temperature controller (Living Systems Instrumentation) and bubbled with 5% CO_2, 20% O_2, and 75% N_2 to maintain the appropriate pH value. Either arterial perfusion pressure (~60 mmHg) or flow rate was kept constant to measure the other parameter. Unless stated otherwise, a constant flow rate was applied in the experiments. The flow rate was set accordingly to make the starting perfusion pressure ~50 to 60 mmHg. The bath solution was perfused at ~5 mL/min. The experimental measurement was started after ~30 min to 1 h stabilization, when the perfusion pressure increased and stabilized at a certain level (~90 to 100 mmHg). For the pacing experiments, the papillary muscle was stabilized and kept at 1 Hz pacing (50 V, 2 ms) for 30 min to 1 h before experiments were performed. When necessary, Alexa Fluor 488- or 633-conjugated WGA (Thermo Fisher Scientific; 20 μg/mL, 30 min) was included in the luminal buffer for the imaging of blood vessels.

Cell Isolation and Culture. Ventricular myocytes from Sprague–Dawley rats were isolated and cultured as described previously (48). Human cardiac microvascular endothelial cells were purchased from Lonza (catalog no. cc-7030) and plated as instructed in the manual provided with the product. In brief, the cryopreserved microvascular endothelial cells (1 mL) were thawed at 37 °C and plated into two 100-mm culture dishes (55 cm^2 surface area) in EGM-2MV medium (cc-3202, Lonza), prewarmed at 37 °C. The cell density was ~5,000 cells/cm^2. The cells from passages six through eight were used in the experiments. EGM-2MV cultural medium supplemented with 2.5% FBS was used in the coculture of endothelial cells and rat ventricular myocytes. The ratio of the ventricular myocyte and the endothelial cells that were plated was ~1:5. The cells were cocultured for no more than 48 h at the time of use in the experiments reported.

Electrophysiology. A conventional whole-cell patch-clamp configuration (Axopatch 200B, Clampex 8.2, Molecular Devices) was used to acquire the whole-cell patch-clamp data. The patch pipette solutions contained 30 mM KCl, 110 K mM aspartic acid, 10 mM NaCl, 1 mM $MgCl_2$, 10 mM Hepes, and 0.05 mM EGTA (pH 7.2 with KOH). The resistance of the pipette was 1.5 to 2 MΩ when filled with pipette solution. The bath solution contained 140 mM NaCl, 10 mM Hepes, 0.5 mM $MgCl_2$, 0.33 mM $NaHPO_4$, 5.5 mM glucose, 1.8 mM $CaCl_2$, and 5 mM KCl (pH 7.4 with NaOH). A whole-cell current clamp configuration was used to measure the membrane potential without injecting any current into the cell. For the whole-cell current recordings, a 500-ms voltage ramp from −140 mV to 40 mV (for endothelial cells) or from 40 mV to −140 mV (for ventricular myocytes) was imposed. All recordings were conducted at room temperature with constant perfusate with Tyrode's solution in the absence (control) or presence of K_{ATP}/Kir2.1 openers and blockers. For the recordings of cocultured cells, 50 μM calcein disodium salt was included in the patch pipette. Data were analyzed offline using Clampfit 10.4. Junction potential was subtracted in the presented data.

Immunostaining. Mouse heart was cannulated and perfused using the Langendorff perfusion system with either Ca^{2+}-free Tyrode's solution or regular Tyrode's solution supplemented with 30 mM BDM at room temperature. WGA (Alexa Fluor 488- or 633-conjugated, 10 μg/mL) and/or Hoechst (10 μM) were loaded for 30 min, followed by a 10-min wash. Then 4% paraformaldehyde (in PBS) was perfused for 15 min to fix the heart, followed by a 5-min wash using PBS. Then the heart was permeabilized using 0.1% or 0.2% Triton X-100 (in PBS) for 15 min. The heart was taken off the Langendorff perfusion rig, and the right ventricular papillary muscles or right ventricle were dissected for whole-mount immunostaining. The tissues were incubated with the primary antibodies anti-NG2 (AB5320, 1:100; Millipore Sigma), anti–α-actinin (A7811, 1:1,000; Sigma), and anti-connexin 43 (C6219, Sigma-Aldrich or MAB3067, EMD Millipore; 1:1,000) over two or three nights at 4 °C in blocking solution (5% goat serum and 0.1% or 0.2% Triton X-100 in phosphate-buffered saline [PBS]), followed by a 2-h wash with PBS. Then the tissues were incubated with an Alexa Fluor-conjugated secondary antibody (1:200 to 1:3,000) for 4 to 6 h at room temperature, followed by an

overnight wash with PBS at 4 °C. The tissues then were either mounted on a Sylgard-coated chamber using a fine needle or glued onto a coverslip and imaged by upright confocal microscopy (Nikon).

Confocal Imaging. Confocal using a Nipkow disk or a point scanning system was used to image the vascular bed and the specific cells (e.g., myocytes, endothelial cells, pericytes, smooth muscle cells) from wild-type, NG2-DsRed, or SMMHKir6.1-AAA mice. The vessels in wild-type or NG2-DsRed mice papillary muscles were loaded with Alexa Fluor 488- or 633-conjugated WGA (20 μg/mL, 30 min) and/or tetramethylrhodamine, methyl ester (TMRM) (10 nM). WGA and TMRM were perfused from the arterial lumen, followed by a 30 min wash. Fluorescence of Alexa fluorophores, DsRed, and TMRM was imaged using inverted (Zeiss) or upright (Nikon) confocal microscopy at 10 to 25 frames per second with a step of 0.5 to 1 μm. To minimize the movement of the sample, some images were taken from the fixed tissue (as stated in the figure legends). The images were analyzed and processed offline. The images in the figures are either reconstructed 3D images or Z projections with maximal fluorescence intensities.

Pressurization of Isolated Mesentery Artery and Data Analysis. For the pressurized mesentery artery experiments, ∼2 to 3 mm of a second-order mesentery artery was dissected and cannulated at both ends, as described previously (49). After stabilization at 10 mmHg for ∼10 min, the luminal pressure was increased and maintained at 70 mmHg. Once tone was developed, K_{ATP} opener pinacidil (100 μM) was applied, followed by application of Ca^{2+} free solution. Acquired data were analyzed offline using ImageJ-win64 (Fiji Is Just ImageJ) and MATLAB (MathWorks) with custom software for diameters.

Chemicals and Statistics. Unless stated otherwise, all of the chemicals were purchased from Sigma-Aldrich. Data were statistically analyzed using the paired *t* test. A *P* value <0.05 was considered to indicate statistical significance.

Data Availability. All data are contained in the main text and *SI Appendix*.

ACKNOWLEDGMENTS. We thank Drs. Colin G. Nichols and Conor McClenaghan (Washington University School of Medicine in St. Louis) for generous advice and for providing the SMMHCKir6.1-AAA mice. This work was supported in part by the Center for Biomedical Engineering and Technology, the NIH (1U01HL116321, 1R01HL142290, and 5UM1 HL120877), the American Heart Association (10SDG4030042, to G.Z. and 19POST34450156, to H.C.J.), the Department of Defense (DoD) (HU0001-18-0016), the European Union Horizon 2020 Research and Innovation Project SVDs@target (Grant Agreement 666881), the National Institute of Neurological Disorders and Stroke and National Institute of Aging (R01 NS110656), and the National Heart, Lung, and Blood Institute (Award R35HL140027).

1. C. B. Wolff, Normal cardiac output, oxygen delivery and oxygen extraction. *Adv. Exp. Med. Biol.* **599**, 169–182 (2007).
2. W. E. Jacobus, Respiratory control and the integration of heart high-energy phosphate metabolism by mitochondrial creatine kinase. *Annu. Rev. Physiol.* **47**, 707–725 (1985).
3. R. Tennant, C. J. Wiggers, The effect of coronary occlusion on myocardial contraction. *Am. J. Physiol.* **112**, 351–361 (1935).
4. R. M. Berne, Cardiac nucleotides in hypoxia: Possible role in regulation of coronary blood flow. *Am. J. Physiol.* **204**, 317–322 (1963).
5. H. J. Knot, P. A. Zimmermann, M. T. Nelson, Extracellular K(+)-induced hyperpolarizations and dilatations of rat coronary and cerebral arteries involve inward rectifier K(+) channels. *J. Physiol.* **492**, 419–430 (1996).
6. A. V. Goodyer, W. F. Eckhardt, R. H. Ostberg, M. J. Goodkind, Effects of metabolic acidosis and alkalosis on coronary blood flow and myocardial metabolism in the intact dog. *Am. J. Physiol.* **200**, 628–632 (1961).
7. A. A. Quyyumi *et al*., Nitric oxide activity in the human coronary circulation. Impact of risk factors for coronary atherosclerosis. *J. Clin. Invest.* **95**, 1747–1755 (1995).
8. S. Saitoh *et al*., Hydrogen peroxide: A feed-forward dilator that couples myocardial metabolism to coronary blood flow. *Arterioscler. Thromb. Vasc. Biol.* **26**, 2614–2621 (2006).
9. E. D. Casalini *et al*., Contribution of hydrogen sulfide to the control of coronary blood flow. *Microcirculation* **21**, 104–111 (2014).
10. A. G. Goodwill, G. M. Dick, A. M. Kiel, J. D. Tune, Regulation of coronary blood flow. *Compr. Physiol.* **7**, 321–382 (2017).
11. D. V. DeFily, W. M. Chilian, Coronary microcirculation: Autoregulation and metabolic control. *Basic Res. Cardiol.* **90**, 112–118 (1995).
12. A. Noma, ATP-regulated K^+ channels in cardiac muscle. *Nature* **305**, 147–148 (1983).
13. T. A. Longden *et al*., Capillary K^+-sensing initiates retrograde hyperpolarization to increase local cerebral blood flow. *Nat. Neurosci.* **20**, 717–726 (2017).
14. V. J. Schouten, C. P. Allaart, N. Westerhof, Effect of perfusion pressure on force of contraction in thin papillary muscles and trabeculae from rat heart. *J. Physiol.* **451**, 585–604 (1992).
15. Q. Aziz *et al*., Molecular and functional characterization of the endothelial ATP-sensitive potassium channel. *J. Biol. Chem.* **292**, 17587–17597 (2017).
16. A. Li *et al*., Hypotension due to Kir6.1 gain-of-function in vascular smooth muscle. *J. Am. Heart Assoc.* **2**, e000365 (2013).
17. A. Morrissey *et al*., Immunolocalization of KATP channel subunits in mouse and rat cardiac myocytes and the coronary vasculature. *BMC Physiol.* **5**, 1 (2005).
18. J. Daut *et al*., Hypoxic dilation of coronary arteries is mediated by ATP-sensitive potassium channels. *Science* **247**, 1341–1344 (1990).
19. C. Bondjers *et al*., Microarray analysis of blood microvessels from PDGF-B and PDGF-Rbeta mutant mice identifies novel markers for brain pericytes. *FASEB J.* **20**, 1703–1705 (2006).
20. D. A. Narmoneva, R. Vukmirovic, M. E. Davis, R. D. Kamm, R. T. Lee, Endothelial cells promote cardiac myocyte survival and spatial reorganization: Implications for cardiac regeneration. *Circulation* **110**, 962–968 (2004).
21. J. M. Beach, E. D. McGahren, B. R. Duling, Capillaries and arterioles are electrically coupled in hamster cheek pouch. *Am. J. Physiol.* **275**, H1489–H1496 (1998).
22. E. Ivanova, T. Kovacs-Oller, B. T. Sagdullaev, Vascular pericyte impairment and Connexin43 gap junction deficit contribute to vasomotor decline in diabetic retinopathy. *J. Neurosci.* **37**, 7580–7594 (2017).
23. S. S. Segal, B. R. Duling, Flow control among microvessels coordinated by intercellular conduction. *Science* **234**, 868–870 (1986).
24. H. L. Kanter, J. E. Saffitz, E. C. Beyer, Cardiac myocytes express multiple gap junction proteins. *Circ. Res.* **70**, 438–444 (1992).
25. K. E. Reed *et al*., Molecular cloning and functional expression of human connexin37, an endothelial cell gap junction protein. *J. Clin. Invest.* **91**, 997–1004 (1993).
26. B. Bastide *et al*., Gap junction protein connexin40 is preferentially expressed in vascular endothelium and conductive bundles of rat myocardium and is increased under hypertensive conditions. *Circ. Res.* **73**, 1138–1149 (1993).
27. J. Flagg-Newton, W. R. Loewenstein, Experimental depression of junctional membrane permeability in mammalian cell culture. A study with tracer molecules in the 300 to 800 Dalton range. *J. Membr. Biol.* **50**, 65–100 (1979).
28. C. G. Nichols, W. J. Lederer, The regulation of ATP-sensitive K^+ channel activity in intact and permeabilized rat ventricular myocytes. *J. Physiol.* **423**, 91–110 (1990).
29. M. Mederos y Schnitzler, C. Derst, J. Daut, R. Preisig-Müller, ATP-sensitive potassium channels in capillaries isolated from guinea pig heart. *J. Physiol.* **525**, 307–317 (2000).
30. J. E. Seiden, O. Platoshyn, A. E. Bakst, S. S. McDaniel, J. X. Yuan, High K(+)-induced membrane depolarization attenuates endothelium-dependent pulmonary vasodilation. *Am. J. Physiol. Lung Cell. Mol. Physiol.* **278**, L261–L267 (2000).
31. G. Edwards, K. A. Dora, M. J. Gardener, C. J. Garland, A. H. Weston, K^+ is an endothelium-derived hyperpolarizing factor in rat arteries. *Nature* **396**, 269–272 (1998).
32. D. Laurent, C. Bolene-Williams, F. L. Williams, L. N. Katz, Effects of heart rate on coronary flow and cardiac oxygen consumption. *Am. J. Physiol.* **185**, 355–364 (1956).
33. K. Garrott *et al*., K_{ATP} channel inhibition blunts electromechanical decline during hypoxia in left ventricular working rabbit hearts. *J. Physiol.* **595**, 3799–3813 (2017).
34. W. J. Lederer *et al*., "Molecular understanding of excitation-contraction coupling and vascular flow control in heart muscle" in *Tissue Oxygen Deprivation: From Molecular to Integrated Function*, G. G. Haddad, G. Lister (Marcel Dekker, New York, 1996), vol. 95, pp. 497–513.
35. V. Ohanyan *et al*., Requisite role of Kv1.5 channels in coronary metabolic dilation. *Circ. Res.* **117**, 612–621 (2015).
36. N. Westerhof, C. Boer, R. R. Lamberts, P. Sipkema, Cross-talk between cardiac muscle and coronary vasculature. *Physiol. Rev.* **86**, 1263–1308 (2006).
37. F. M. O'Farrell *et al*., Capillary pericytes mediate coronary no-reflow after myocardial ischaemia. *eLife* **6**, e29280 (2017).
38. K. W. Zimmermann, Der feinere bau der blutkapillaren. *Z. Anat. Entwicklungsgesch.* **68**, 29–109 (1923).
39. M. T. Nelson *et al*., Relaxation of arterial smooth muscle by calcium sparks. *Science* **270**, 633–637 (1995).
40. M. P. Wiedeman, R. F. Tuma, H. N. Mayrovitz, Defining the precapillary sphincter. *Microvasc. Res.* **12**, 71–75 (1976).
41. T. Saito, T. Sato, T. Miki, S. Seino, H. Nakaya, Role of ATP-sensitive K^+ channels in electrophysiological alterations during myocardial ischemia: A study using Kir6.2-null mice. *Am. J. Physiol. Heart Circ. Physiol.* **288**, H352–H357 (2005).
42. T. Burdyga, L. Borysova, Ca^{2+} signalling in pericytes. *Adv. Exp. Med. Biol.* **1109**, 95–109 (2018).
43. C. N. Hall *et al*., Capillary pericytes regulate cerebral blood flow in health and disease. *Nature* **508**, 55–60 (2014).
44. U. Langheinrich, J. Daut, Hyperpolarization of isolated capillaries from guinea-pig heart induced by K^+ channel openers and glucose deprivation. *J. Physiol.* **502**, 397–408 (1997).
45. C. G. Nichols, W. J. Lederer, Adenosine triphosphate-sensitive potassium channels in the cardiovascular system. *Am. J. Physiol.* **261**, H1675–H1686 (1991).
46. M. C. Sanguinetti, A. L. Scott, G. J. Zingaro, P. K. Siegl, BRL 34915 (cromakalim) activates ATP-sensitive K^+ current in cardiac muscle. *Proc. Natl. Acad. Sci. U.S.A.* **85**, 8360–8364 (1988).
47. M. Suzuki *et al*., Role of sarcolemmal K(ATP) channels in cardioprotection against ischemia/reperfusion injury in mice. *J. Clin. Invest.* **109**, 509–516 (2002).
48. G. Zhao, T. Li, D. X. Brochet, P. B. Rosenberg, W. J. Lederer, STIM1 enhances SR Ca^{2+} content through binding phospholamban in rat ventricular myocytes. *Proc. Natl. Acad. Sci. U.S.A.* **112**, E4792–E4801 (2015).
49. A. Adebiyi, G. Zhao, S. Y. Cheranov, A. Ahmed, J. H. Jaggar, Caveolin-1 abolishment attenuates the myogenic response in murine cerebral arteries. *Am. J. Physiol. Heart Circ. Physiol.* **292**, H1584–H1592 (2007).